Supplementary manuscript

Title: Androgen Signaling Represses Homeobox C9, an Inhibitor of Androgen Receptor, in Prostate Cancer Cells

Authors and affiliations:

Takao Susa[1*], Eiki Tsuboi[1], Tomoko Okada[1], Miho Akimoto[1], Noriyuki Okudaira[1], Hiroko Okinaga[2], Masayoshi Iizuka[1, 3], Tomoki Okazaki[1], and Mimi Tamamori-Adachi[1]

1 Department of Biochemistry, Teikyo University School of Medicine, Tokyo, Japan

2 Department of Internal Medicine, Teikyo University School of Medicine, Tokyo, Japan

3 Medical Education Centre, Teikyo University School of Medicine, Tokyo, Japan.

∗ Corresponding author

∗ Correspondence:

Takao Susa

Department of Biochemistry, Teikyo University School of Medicine

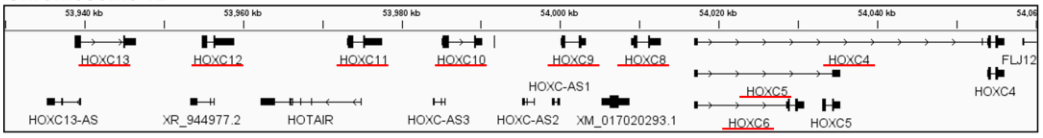
2-11-1 Kaga, Itabashi-Ku, Tokyo 173-8605, Japan

Phone and fax number: +81 3 3964 3649

Email address: tsusa@med.teikyo-u.ac.jp; susa.takao.ty@teikyo-u.ac.jp

This file including Supplemental Figures S1-S8 and Supplemental Tables S1-S9.

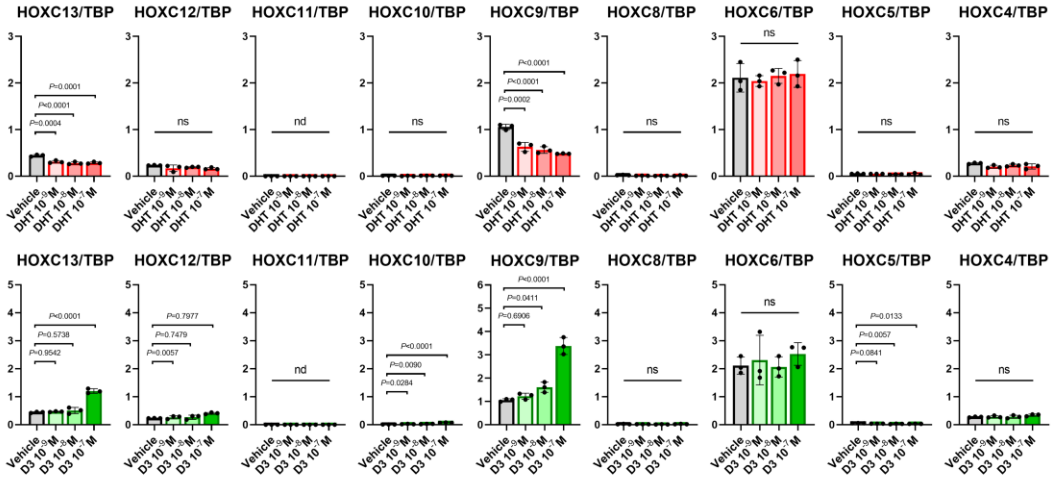
(a)



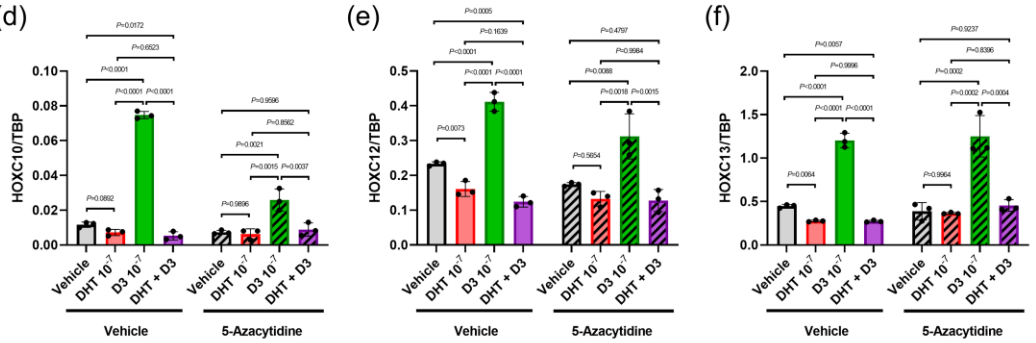
(b)

Gene Symbol	Microarray Signal			Ratio	
	Vehicle(V)	DHT	D3	DHT/V	D3/V
HOXC4	337	216	634	0.6	1.9
HOXC5	26	10	15	0.4	0.6
HOXC6	5850	4399	6692	0.8	1.1
HOXC8	46	5	39	0.1	0.8
HOXC9	2843	1010	7863	0.4	2.8
HOXC10	8	5	13	0.6	1.6
HOXC11	5	5	5	1.0	1.0
HOXC12	686	452	1026	0.7	1.5
HOXC13	628	339	1620	0.5	2.6

(c)



(d) (e) (f)

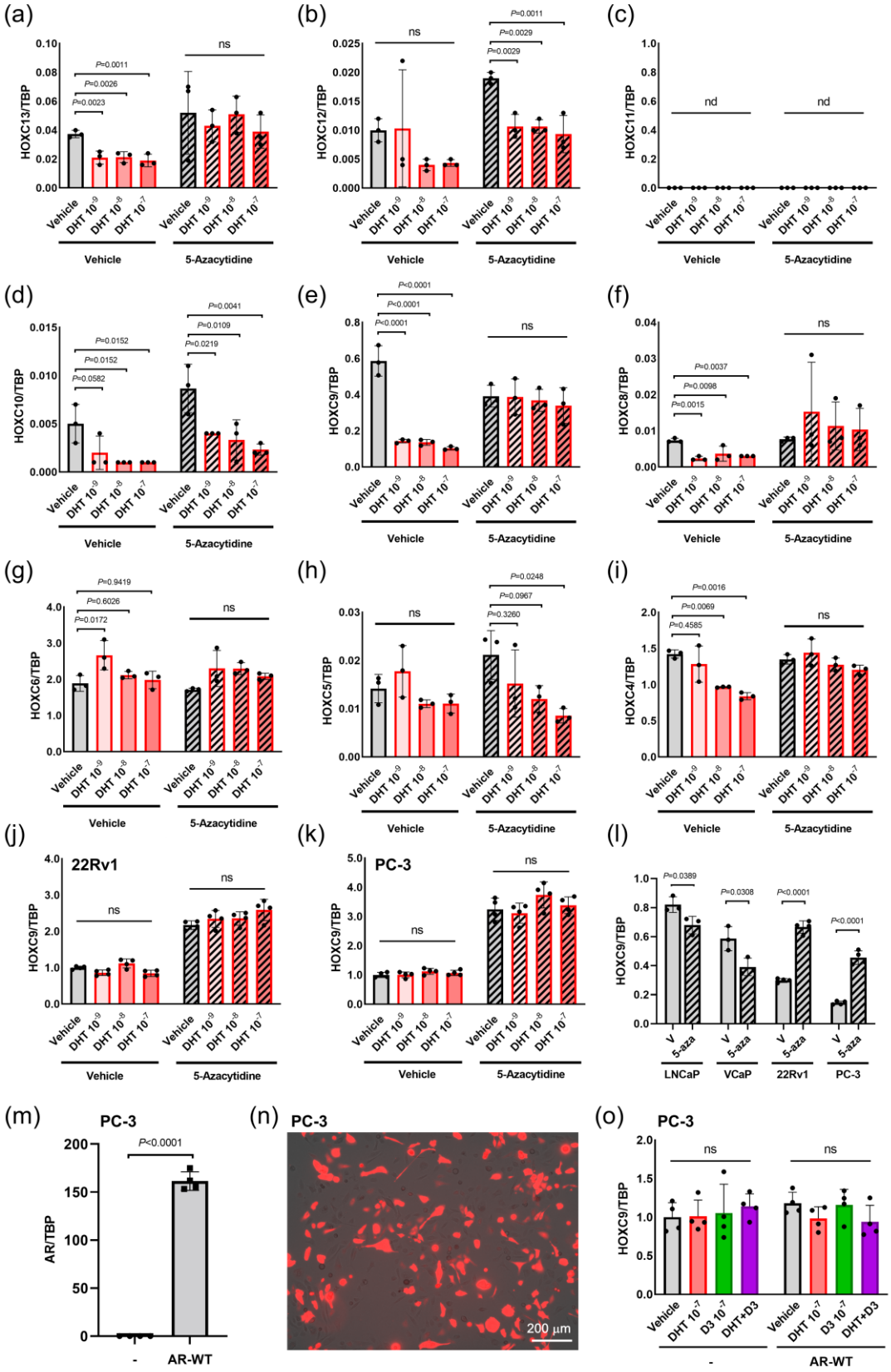


Supplementary Figure S1

The *HOXC* gene cluster is regulated by DHT and D3 in LNCaP cells.

(a) The *HOXC* gene cluster comprises nine genes (*HOXC4–6* and *8–13*) and is located at human chromosome 12q12–q13. (b) *HOXC* gene regulation by DHT and D3: from microarray data

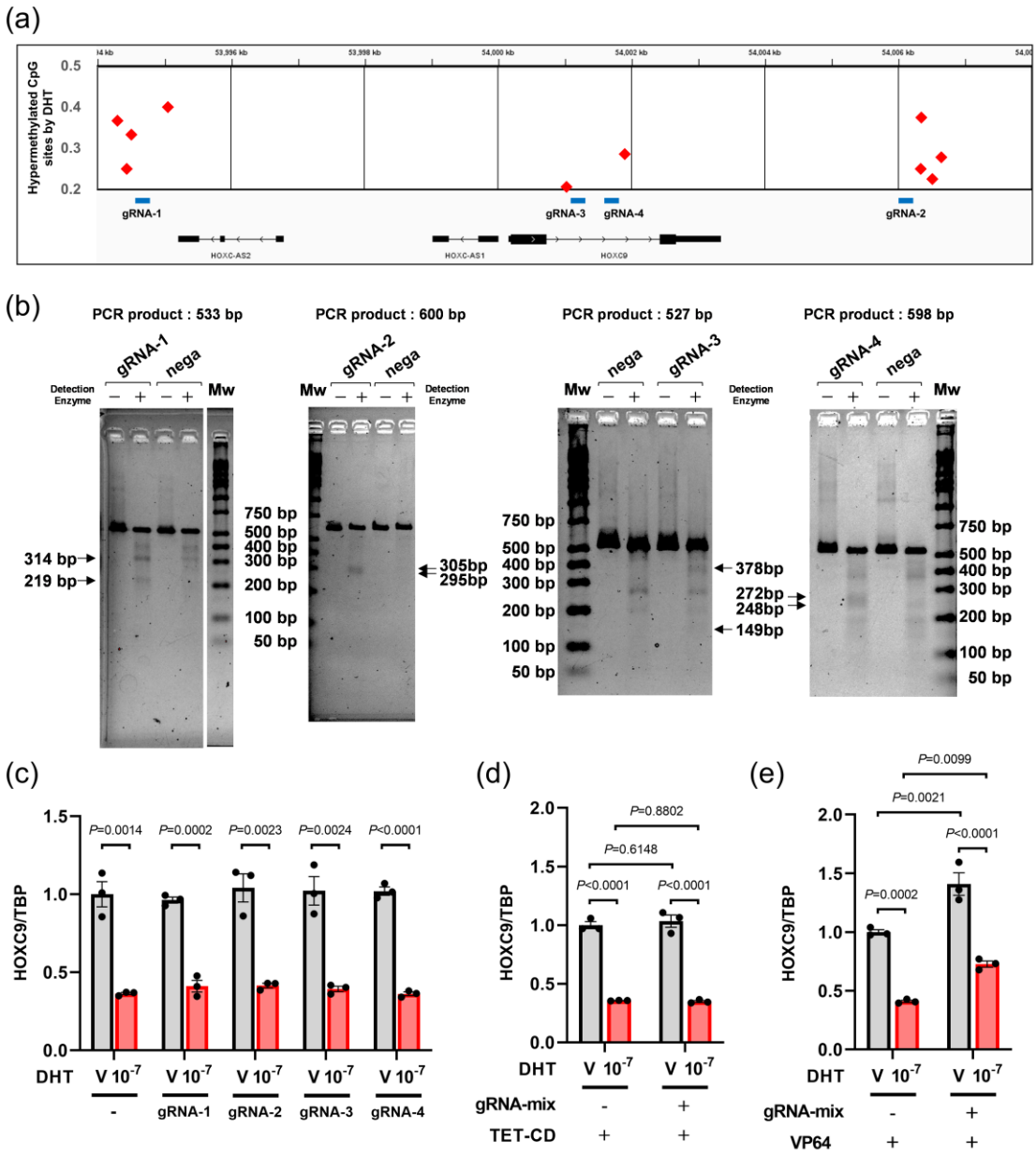
showing variation in expression in LNCaP cells treated with DHT and D3. Opposing gene regulation by DHT and D3 was observed in not only *HOXC9* but also other HOXC family genes. (c) qRT-PCR analysis showing regulation of *HOXC4–6* and *8–13* by DHT and D3 confirmed an opposite trend of regulation of *HOXC13* in addition to *HOXC9*. qRT-PCR analysis of *HOXC10* (D), *11* (E), and *13* (F) gene regulation by 10^{-7} M DHT, D3, and DHT and D3 with and without preadministration of 10^{-5} M 5-azacytidine. Data were normalized to *TBP* expression. Data are presented as means ± SD ($n = 3$). ns and nd indicates not significant and not detection.


(a)
HOXC13/TBP
P=0.0011
P=0.0026
P=0.0023
ns
(b)
HOXC12/TBP
ns
P=0.0011
P=0.0029
P=0.0029
(c)
HOXC11/TBP
nd
nd
(d)
HOXC10/TBP
P=0.0152
P=0.0152
P=0.0582
P=0.0041
P=0.0109
P=0.0219
(e)
HOXC9/TBP
P<0.0001
P<0.0001
P<0.0001
ns
(f)
HOXC8/TBP
P=0.0037
P=0.0098
P=0.0015
ns
(g)
HOXC6/TBP
P=0.9419
P=0.6026
P=0.0172
ns
(h)
HOXC5/TBP
ns
P=0.0248
P=0.0967
P=0.3260
(i)
HOXC4/TBP
P=0.0016
P=0.0069
P=0.4585
ns
Vehicle
DHT 10-9
DHT 10-8
DHT 10-7
Vehicle
5-Azacytidine
(j)
22Rv1
HOXC9/TBP
ns
ns
(k)
PC-3
HOXC9/TBP
ns
ns
(l)
HOXC9/TBP
P=0.0389
P=0.0308
P<0.0001
P<0.0001
V
5-aza
LNCaP
VCaP
22Rv1
PC-3
(m)
PC-3
AR/TBP
P<0.0001
-
AR-WT
(n)
PC-3
200 µm
(o)
PC-3
HOXC9/TBP
ns
ns
Vehicle
DHT 10-7
D3 10-7
DHT+D3
-
AR-WT

Supplementary Figure S2

DHT-dependent repression of *HOXC* cluster genes in other human prostate cancer cell lines (VCaP, 22Rv1, and PC-3).

HOXC13 (a), *12* (b), *11* (c), *10* (d), *9* (e), *8* (f), *6* (g), *5* (h), and *4* (i) expression in VCaP cells when 10^{-5} M 5-azacytidine or vehicle was administered before DHT. The same conditions of *HOXC9* expression were analyzed in 22Rv1 (j) and PC-3 (k) cells. (l) Comparison of the relative expression of *HOXC9* toward that of *TBP* in LNCaP, VCaP, 22Rv1, and PC-3 cells treated with the vehicle or 10^{-5} M 5-azacytidine. (m) qRT-PCR analysis of *AR* expression following high-efficiency Neon transfection of wild-type *AR* (AR-WT) in PC-3 cells. (n) PC-3 cells expressing DsRed under the same transfection conditions as (m) and (o). Merged images of DsRed fluorescence and bright-field. Scale: 100 μm. (o) Responses of *HOXC9* gene expression to DHT and D3 following Neon-mediated transfection of AR-WT in PC-3 cells. Empty vector is indicated as "-" (m and o). qRT-PCR data were normalized to *TBP* expression. Data are presented as relative expression to each *TBP* expression (a–m and o). Data are presented as means ± SD ($n = 3$ for a–l and, $n = 4$ for m and o). V, 5-aza, ns, and nd indicates vehicle, 5-azacytidine, not significant, and not detection, respectively.

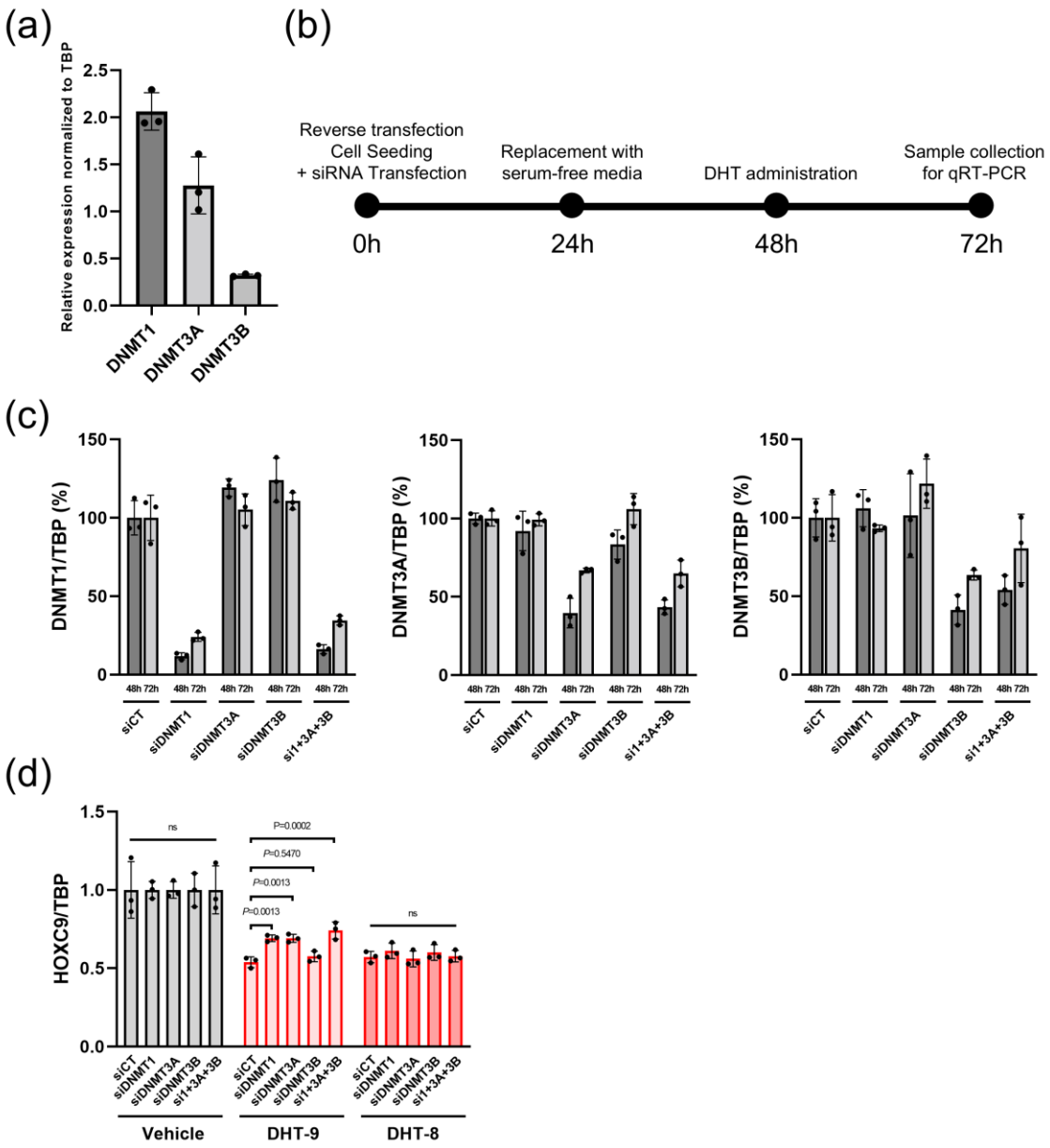


Supplementary Figure S3

Targeted demethylation and activation of *HOXC9* using the CRISPR–dCas9–SunTag platform in LNCaP cells.

(a) Hypermethylated CpG sites around the *HOXC9* gene−four sites in the upstream region from *HOXC9*, two sites in the first intron, and four sites in the downstream region—are indicated by red dots. Blue lines show the location of gRNA-1–4. Sequences of gRNAs are shown in Supplementary Table S8. (b) The quality of the designed gRNAs was evaluated using GeneArt

Genomic Cleavage Detection Kit. Genomic PCR product and PCR fragment sizes digested by the detection enzyme are shown in Supplementary Table S9. The analysis of PCR products amplified from LNCaP cells transfected without gRNAs are shown as nega. (c) At 48 h after transfection of pCAG-dCas9-5xPlat2Af1D, pCAG-scFvGCN4sfGFPTET1CD, and respective gRNA expression vectors into LNCaP cells, the cells were administered 10^{-7} M DHT. qRT-PCR was used to analyze *HOXC9* expression. (d) Similar experiment to (c) was performed with a mixture of gRNA-1–4. (e) Similar experiment to (d) was performed replacing pCAG-scFvGCN4sfGFPTET1CD with pCAG-scFvGCN4sfGFP-VP64-GB1. qRT-PCR data were normalized to *TBP* expression and are presented as relative expression to the vehicle of no-gRNA introducing. Data are presented as means ± SD ($n = 3$).

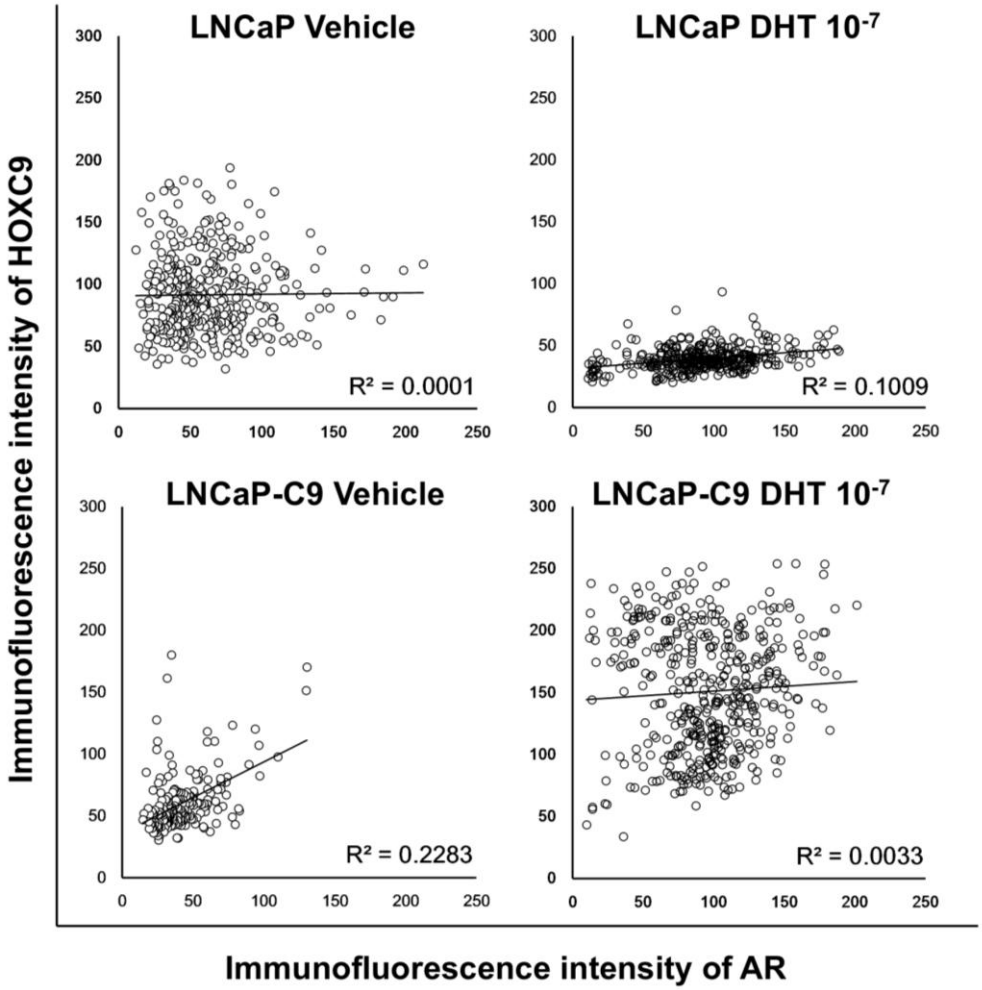


Supplementary Figure S4

Involvement of DNMTs in androgen-dependent repression of *HOXC9* in LNCaP cells.

(a) qRT-PCR analyses of *DNMT1*, *DNMT3A*, and *DNMT3B* in LNCaP cells. (b) Experimental scheme illustrating siRNA reverse transfection, DHT treatment, and sampling in LNCaP cells. This protocol required 72 h from siRNA transfection to qRT-PCR sample collection. (c)

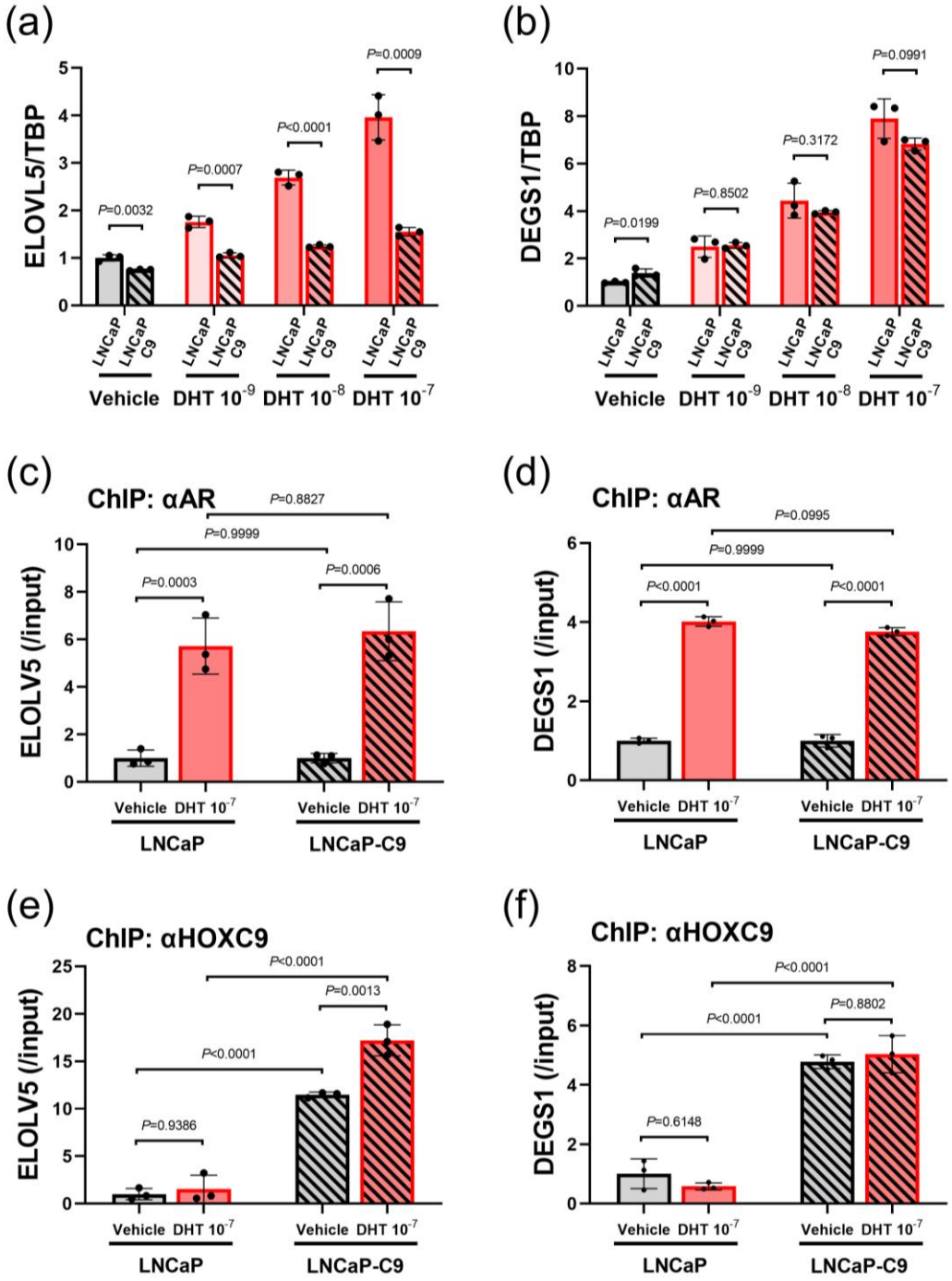
Negative control siRNA (siCT), *DNMT1* siRNA (siDNMT1), *DNMT3A* siRNA (siDNMT3A), *DNMT3B* siRNA (siDNMT3B), or a mixture of *DNMT1*, *DNMT3A*, and *DNMT3B* siRNAs (si1+3A+3B) were transfected into LNCaP cells as described in (b). At 48 h and 72 h after transfection, *DNMT1*, *DNMT3A*, and *DNMT3B* expression was analyzed by qRT-PCR. Expression relative to each siCT is shown. (d) At 24 h after siRNA transfection, the culture medium of LNCaP cells was changed to serum-free medium for 24 h. The cells were then treated with DHT at 10^{-9} M or 10^{-8} M for an additional 24 h, after which *HOXC9* expression was analyzed by qRT-PCR as described in (b). Accordingly, *HOXC9* expression in LNCaP cells was analyzed 72 h post-siRNA transfection. (a,c,d) Data were normalized to *TBP* expression. Data are presented as means ± SD ($n = 3$). (g) Data are presented as means ± SD (n = 3 for (a) and (b), and $n = 4$ for (d)).



Supplementary Figure S5

Immunofluorescence intensities of AR and HOXC9 in individual LNCaP and LNCaP-C9 cells.

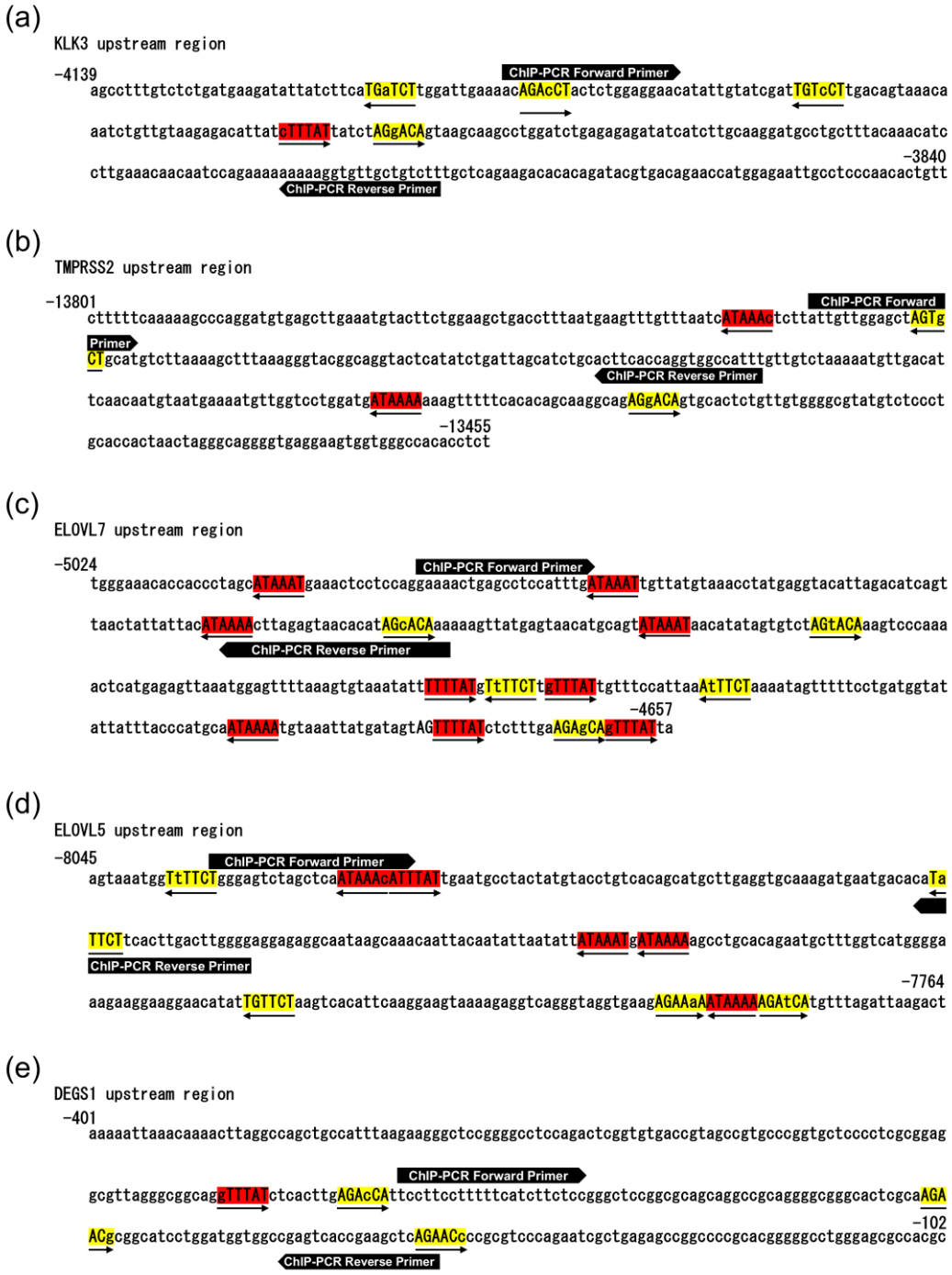
Scatter plots showing the immunofluorescence intensities of AR and HOXC9 in individual LNCaP and LNCaP-C9 cells (Figure 4c). R^2 values for each fitted line are shown.



Supplementary Figure S6

qRT-PCR and ChIP-qPCR analyses of selected AR target genes of *ELOVL5* and *DEGS1* in LNCaP and LNCap-C9 cells.

Comparative qRT-PCR and ChIP-qPCR analyses of *ELOVL5* and *DEGS1* between LNCaP and LNCaP-C9 cells when DHT was administered. Gene expression analyses for *ELOVL5* (a) and *DEGS1* (b) by qRT-PCR. Data were normalized to *TBP* expression and are presented as relative to the vehicle in LNCaP cells ($n = 3 \pm$ SD). ChIP-qPCR analyses utilizing αAR and αHOXC9 antibodies for the AR-binding sites located at the flanking regions of *ELOVL5* (c and e) and *DEGS1* (d and f), respectively. Data are presented as relative to the result using each input DNA ($n = 3 \pm$ SD).



Supplementary Figure S7

Consensus sequences for the AR half-site and HOXC9 around the AR-binding regions analyzed by ChIP-PCR.

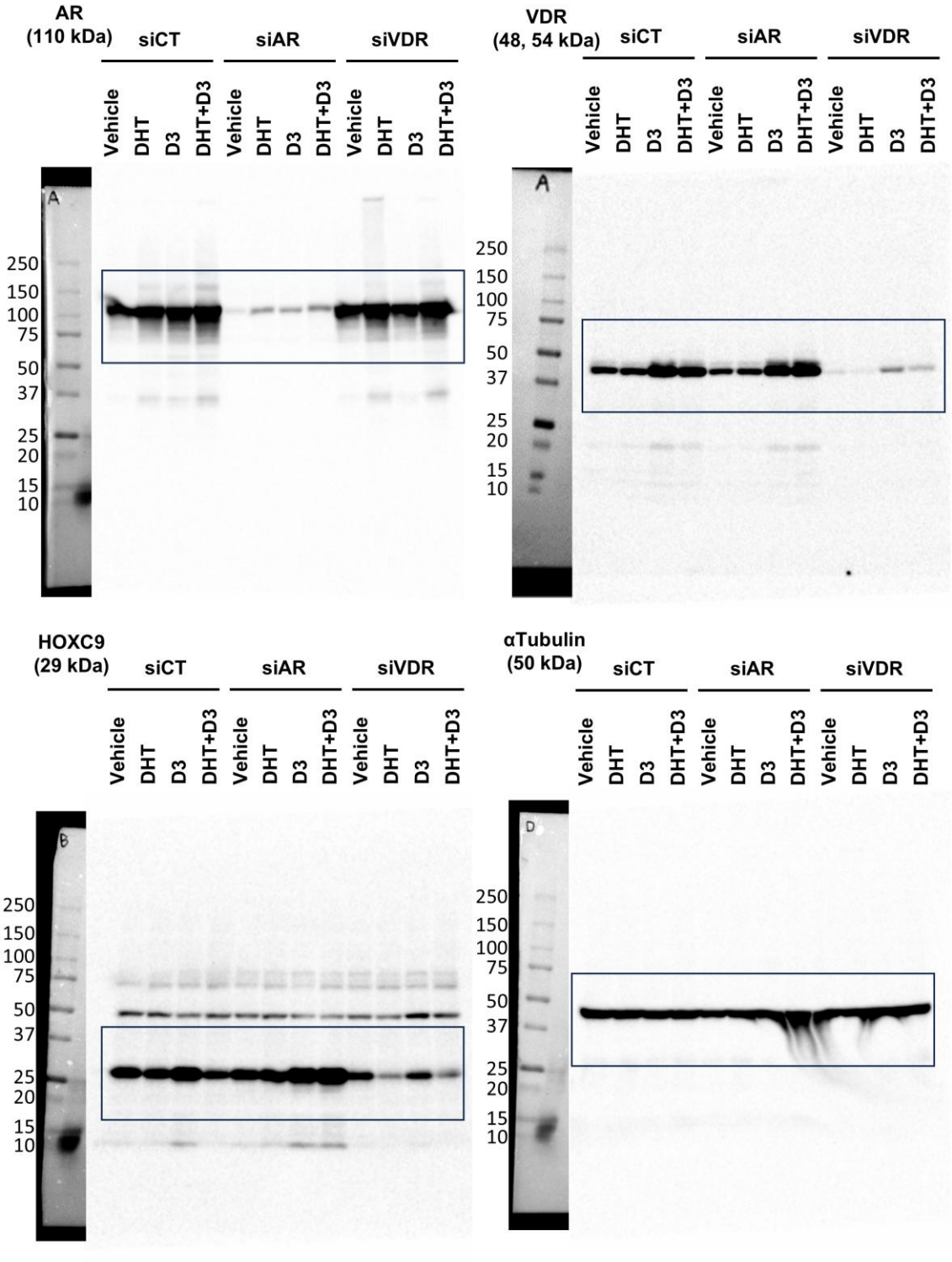
The sequences of the upstream region of *KLK3* (a), *TMPRSS2* (b), *ELOLV7* (c), *ELOLV5* (d), and *DEGS1* (e) amplified by ChIP-PCR. The sites are registered as AR-binding region in the

ChIP-Atlas database. Primers used for amplification of ChIP-qPCR are indicated with big arrows. The candidate binding sequences of AR (similar sequence to AGAACT/A that has a consensus sequence of the AR half-site) and HOXC9 (similar sequence to T/ATTTAT) are shown with yellow and red backgrounds with each direction, respectively, and the directions of the sequences are indicated by arrows.

Supplementary Figure S8

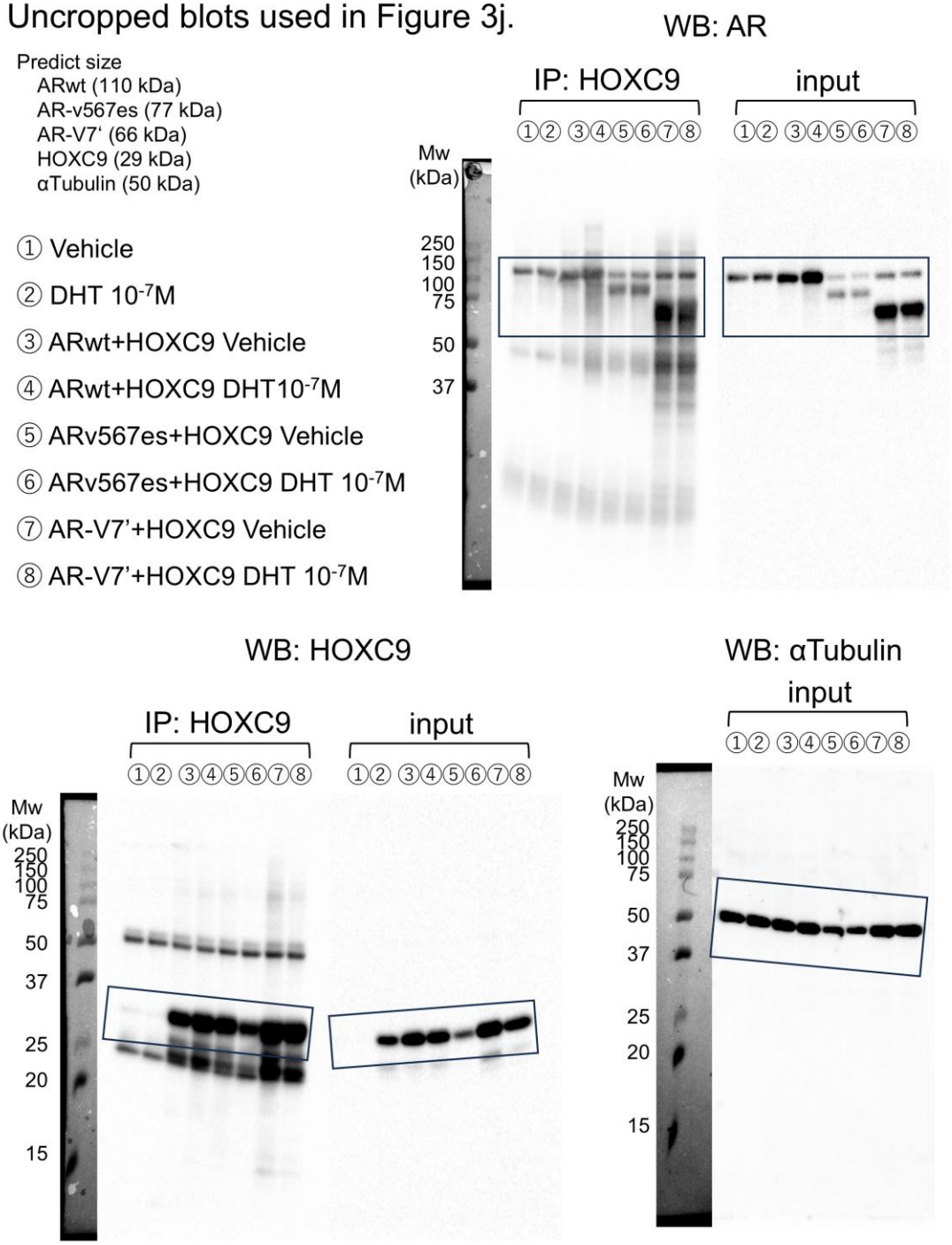
Uncropped blots used in Figure 1f.

Predict size
AR (110 kDa), VDR (48,54 kDa)
HOXC9 (29 kDa), αTubulin (50 kDa)



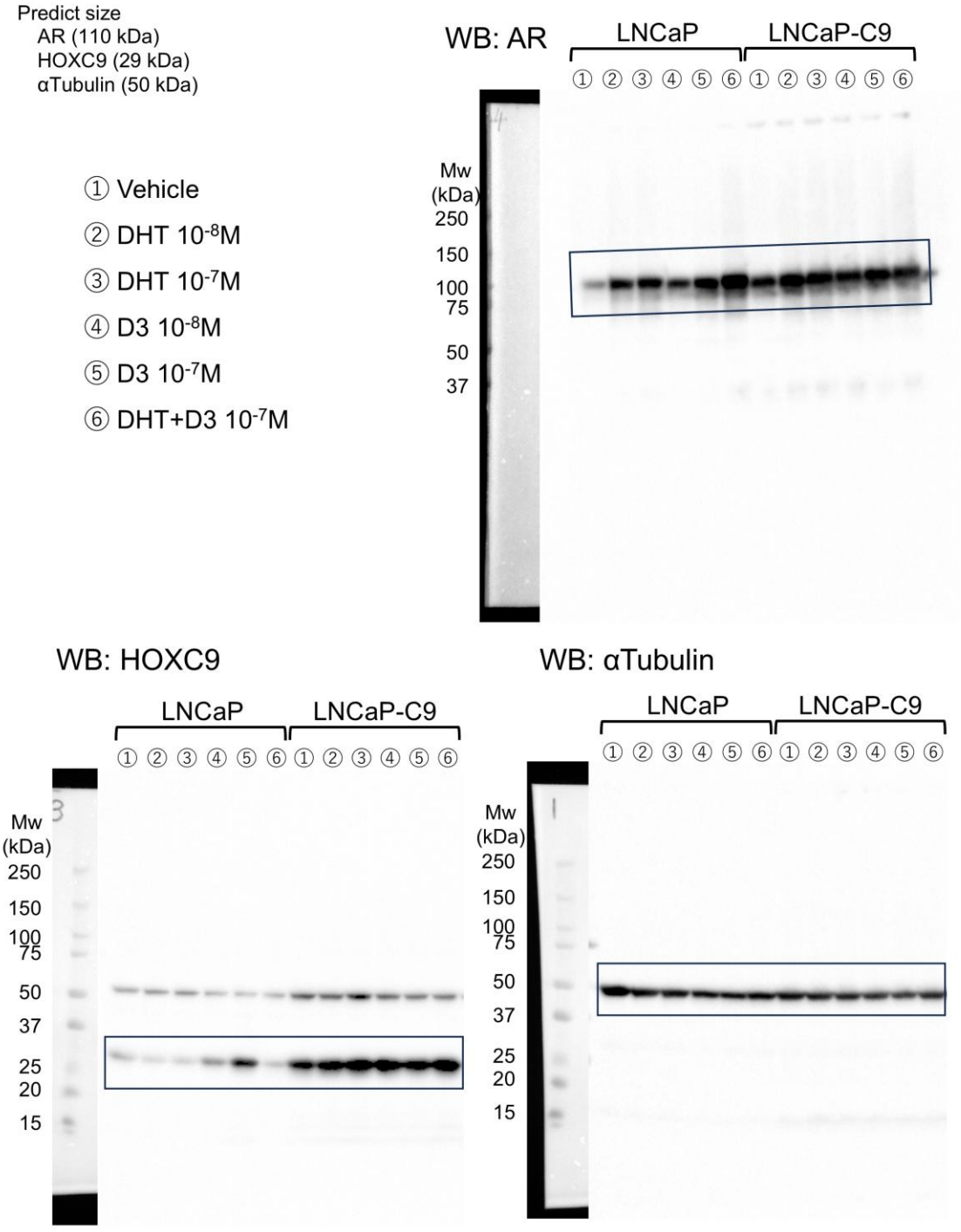
Supplementary Figure S8

Uncropped blots used in Figure 3j.



Supplementary Figure S8

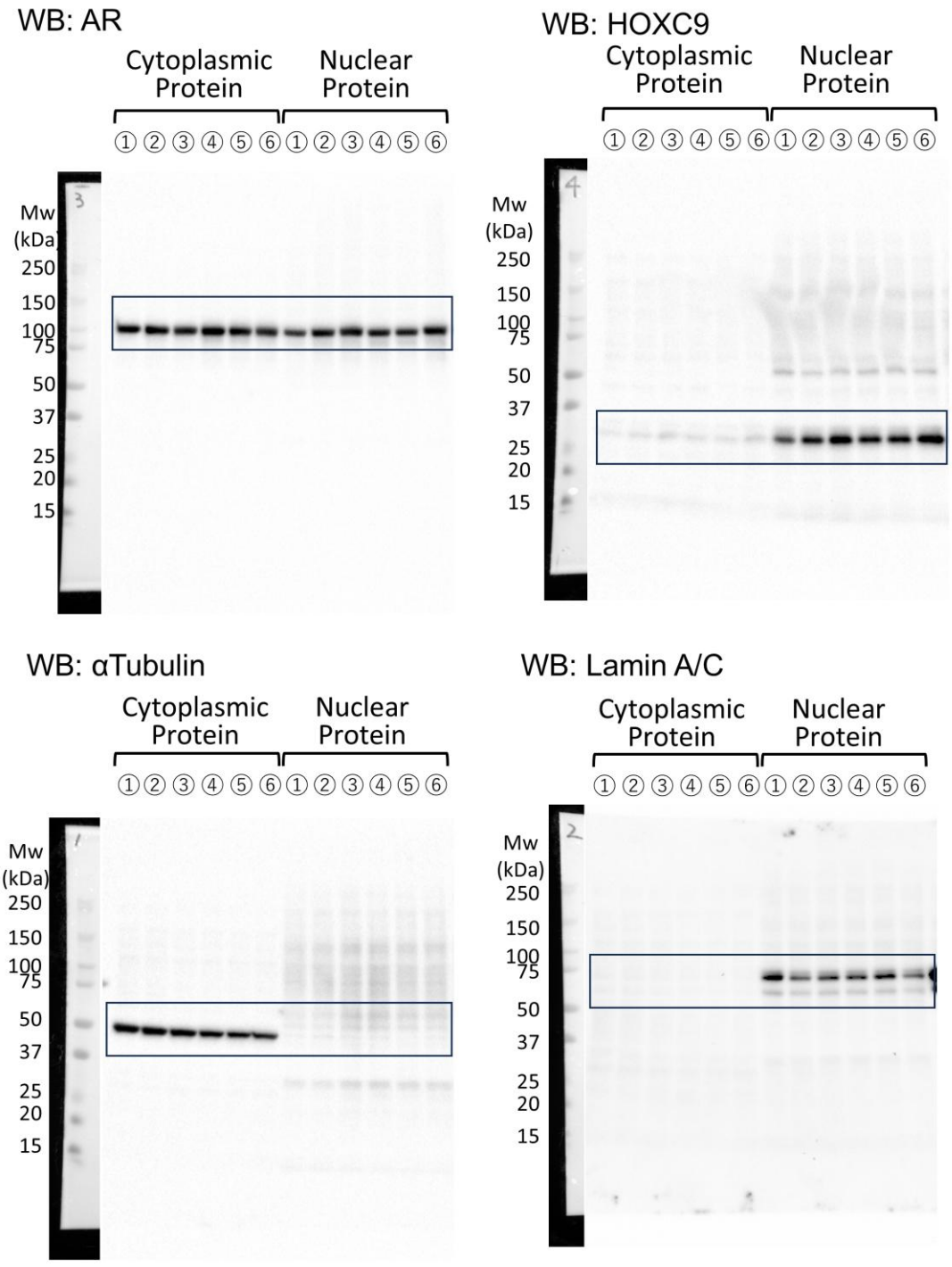
Uncropped blots used in Figure 4b (Whole Protein).



Supplementary Figure S8

Uncropped blots used in Figure 4b (Cytoplasmic and Nuclear Protein).

Predict size
AR (110 kDa), HOXC9 (29 kDa), αTubulin (50 kDa), LaminA/C (LaminA: 74 kDa and LaminC: 63 kDa)

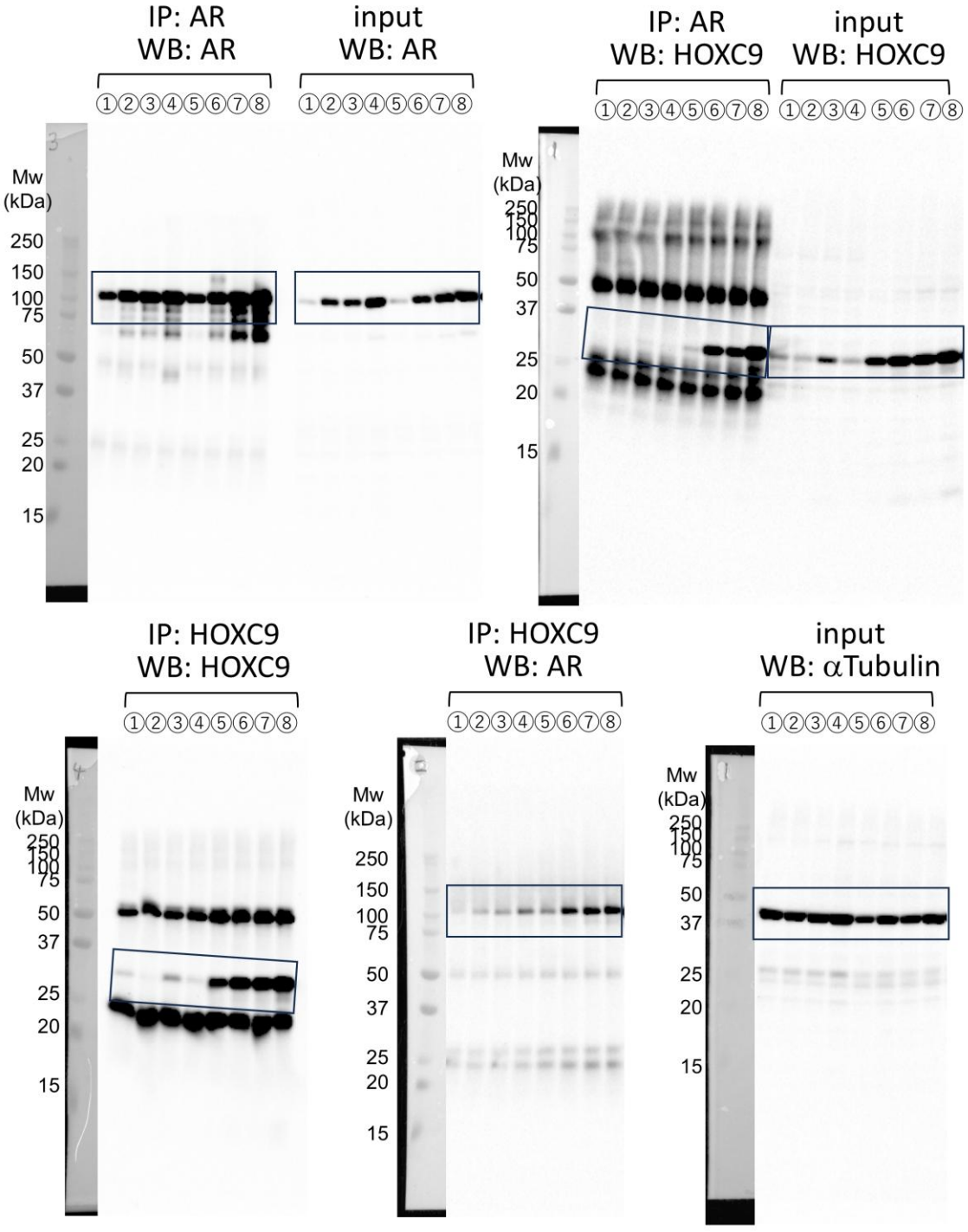


Supplementary Figure S8

Uncropped blots used in Figure 4e.

Predict size
AR (110 kDa), HOXC9 (29 kDa), αTubulin (50 kDa)

① LNCaP Vehicle
② LNCaP DHT 10^{-7}M
③ LNCaP D3 10^{-7}M
④ LNCaP DHT+D3 10^{-7}M
⑤ LNCaP-C9 Vehicle
⑥ LNCaP-C9 DHT 10^{-7}M
⑦ LNCaP-C9 D3 10^{-7}M
⑧ LNCaP-C9 DHT+D3 10^{-7}M



Supplementary Table S1. Primer sets used for qRT-PCR.

Gene	Forward	Reverse
AR	cctggcttccgcaacttacac	ggacttgtgcatgcggtactc
VDR	cactattcacctgccccttc	ctccctccaccatcattcac
HOXC4	caagcaacccatagtctacc	gtataggctgtcctcgagcg
HOXC5	ccgccacagatttacc	agtctggtagcgcgtgtaa
HOXC6	cagatttacccctggatg	ggtctggtaccgcgagtaga
HOXC8	actcgtctcccagcctcat	caaggtctgataccggctgt
HOXC9	ggcagcaagcacaaagag	cagcgcttcttcctcgtg
HOXC10	actccagcccagacacctc	cctcttcttccttccgctct
HOXC11	aacacaaatcccagctcgtc	ataagggcagcgcttcttg
HOXC12	agcttggtatcgccgttgaa	ttcgaatagggcttgcgctt
HOXC13	ccacctctggaagtctccct	tgcaccttagtgtagggcac
KLK3 (PSA)	tctgcggcggtgttctg	gccgacccagcaagatca
TMPRSS2	tgatggtattcacggactgg	cagccccattgttttcttg
ELOVL7	ggccagcctaccagaagtatt	agaactggcttatgtggatgg
ELOVL5	cacattccctcttggttggt	gaggccccttttcttgttgta
DEGS1	ccctggcacaatttcagagt	tcctgtgagtgaaactgagca
DNMT1	agtacctggacgaccctgac	ttggcatcaaagatggacag
DNMT3A	gggcaaagaccagcatttt	agtggactgggaaaccaaat
DNMT3B	ccatgcaacgatctctcaaa	gggcgtgagtaattcagcag

Supplementary Table S2. siRNA sequences.

Gene	siRNA-1	siRNA-2	siRNA-3	siRNA-4
Non-targeting control siRNA	UAGCGACUAAACACAUCAA	UAAGGCUAUGAAGAGAUAC	AUGUAUUGGCCUGUAUUAG	AUGAACGUGAAUUGCUCAA
AR	GGAACUCGAUCGUAUCAUU	UCAAGGAACUCGAUCGUAU	GAAAUGAUUGCACUAUUGA	CGUGCAGCCUAUUGCGAGA
VDR	GCAACCAAGACUACAAGUA	UCAAUGCUAUGACCUGUGA	CCAUUGAGGUCAUCAUGUU	UAGAGAUAUGGCAGCGAAA
DNMT1	GGAAGAAGAGUUACUAUAA	GAGCGGAGGUGUCCCAAUA	GGACGACCCUGACCUCAAA	GAACGGUGCUCAUGCUUAC
DNMT3A	GCAUUCAGGUGGACCGCUA	GCACUGAAAUGGAAAGGGU	CUCAGGCGCCUCAGAGCUA	GGGACUUGGAGAAGCGGAG
DNMT3B	GAAAGUACGUCGCUUCUGA	ACAAAUGGCUUCAGAUGUU	GCUCUUACCUUACCAUCGA	UUUACCACCUGCUGAAUUA

Supplementary Table S3. Primer sets used for ChIP-PCR.

Gene	Forward	Reverse
HOXC9	tttctcctgttcctccgttg	tgaggatcatttgattgttcata
KLK3(PSA)	acagacctactctggaggaac	aagacagcaacacctttt
TMPRSS2	attgttggagctagtgctgcat	aaatggccacctggtgaagt
ELOVL7	gaaaacagagcctccatttga	tttgtgctatgtgttactctaagtttt
ELOVL5	tgggagtctagctcaataaacatt	ccccaagtcaagtgaagaatatg
DEGS1	tccttccttttcatcttctcc	tctgagcttcggtgactcg

Supplementary Table S4. Primer sets used for the expression vector construction.

Gene	Forward	Reverse
HOXC9 (CDS)	agcatgtcggcgacggggcccatc	ttaggactgctccttgtcggttttc
AR-v567es (for inverse PCR)	attgcgagagagctgcatcagt	caggcaaggccttggcccac
AR-V7' (for inverse PCR)	attgcgagagagctgcatcagt	ctcccagagtcatccctgcttc

Supplementary Table S5. Thirty-five common target genes shared by DHT and D3 in LNCaP cells.

ProbeID	GeneSymbol	DHT/V-ratio	DHT/V-Zscore	D3/V-ratio	D3/V-Zscore	V_signal	DHT_signal	D3_signal	V_flag	DHT_flag	D3_flag	GenbankAccession
A_23_P29067	TMPRSS2	32.6	10.3	23.8	23.2	1046	34080	24893	P	P	P	NM_005656
A_21_P0012332		15.8	7.3	2.7	7.2	2502	39454	6645	P	P	P	
A_21_P0011196		15.7	8.1	2.4	6.0	696	10954	1669	P	P	P	
A_23_P500353	KCNN2	13.3	7.7	11.6	16.8	475	6344	5494	P	P	P	NM_021614
A_21_P0012331		13.3	6.9	2.4	8.0	5072	67539	12409	P	P	P	
A_21_P0012330		12.8	6.8	2.5	6.7	4074	52073	10142	P	P	P	
A_23_P119778	SLC39A10	9.2	6.6	2.8	4.7	229	2121	634	P	P	P	NM_020342
A_23_P31407	AGR2	3.9	4.0	0.4	-6.4	891	3509	351	P	P	P	NM_006408
A_21_P0012089	FAR2P1	3.6	3.8	2.4	4.0	257	937	610	P	P	P	NR_026758
A_23_P213085	SLC10A7	3.5	3.7	2.1	3.4	234	828	490	P	P	P	NM_001029998
A_23_P19624	BMP6	3.5	3.7	2.0	3.3	277	975	564	P	P	P	NM_001718
A_23_P136671	UGT2B7	3.1	3.4	0.4	-7.1	1843	5793	656	P	P	P	NM_001074
A_23_P409623	PPFIBP2	2.9	3.2	2.5	6.3	549	1602	1363	P	P	P	NM_003621
A_23_P420348	POTED	2.9	2.4	2.8	4.7	114	329	321	P	P	P	NM_174981
A_24_P825874	POTEI	2.8	3.1	2.2	5.5	323	914	714	P	P	P	NM_001277406
A_23_P315836	BAIAP2	2.8	2.3	2.8	4.7	147	411	411	P	P	P	NM_017451
A_33_P3342957	STK17B	2.7	2.3	3.3	5.5	105	288	349	P	P	P	NM_004226
A_23_P138665	GLUD1	2.7	2.9	2.0	5.1	2653	7129	5344	P	P	P	NM_005271
A_24_P252497	TRIB1	0.5	-2.1	2.1	6.8	6285	3132	13411	P	P	P	NM_025195
A_23_P210581	KCNG1	0.4	-2.7	2.3	5.7	1016	408	2319	P	P	P	NM_002237
A_32_P78783	ZNF778	0.4	-2.1	0.4	-4.6	382	151	142	P	P	P	NM_001201407
A_23_P402610	PFAS	0.4	-2.1	0.5	-3.4	520	205	247	P	P	P	NM_012393
A_21_P0010925		0.4	-2.2	0.3	-5.3	501	192	160	P	P	P	
A_23_P25150	HOXC9	0.4	-3.1	2.8	7.4	2843	1010	7863	P	P	P	NM_006897
A_21_P0000740	HIVEP3	0.3	-3.2	0.2	-7.5	783	268	153	P	P	P	NR_038260
A_23_P23815	SLC30A1	0.3	-2.4	0.5	-3.4	577	197	275	P	P	P	NM_021194
A_33_P3258223	MCM7	0.3	-2.5	0.3	-5.1	536	174	175	P	P	P	NM_005916
A_33_P3315314	MT1HL1	0.2	-4.7	0.3	-8.8	8004	1647	2409	P	P	P	NM_001276687
A_33_P3231156		0.2	-3.7	0.3	-5.4	588	117	183	P	P	P	
A_33_P3350056	MT1X	0.2	-4.8	0.4	-7.6	6747	1329	2397	P	P	P	NM_005952
A_23_P37983	MT1B	0.2	-5.1	0.3	-9.8	9611	1728	2503	P	P	P	NM_005947
A_23_P427703	MT1L	0.2	-5.4	0.2	-10.7	9876	1585	2293	P	P	P	NR_001447
A_23_P106844	MT2A	0.2	-4.9	0.3	-11.7	32012	5093	8682	P	P	P	NM_005953
A_23_P206724	MT1E	0.2	-5.5	0.2	-10.7	8000	1247	1862	P	P	P	NM_175617
A_33_P3233645	MT1G	0.1	-5.8	0.2	-11.8	11985	1664	2398	P	P	P	NM_005950
A_23_P15174	MT1F	0.1	-6.0	0.2	-10.2	3795	508	946	P	P	P	NM_005949

Supplementary Table S6. DHT induced DNA hypermethylated CpG sites around the HOXC locus in LNCaP cells.

TargetID	Vehicle	DHT	DHT-Vehicle, delta_mean	DHT-Vehicle, comment	Vehicle, coverage	DHT, coverage	Chrom	Pos	Strand	Promoter_gene_id	Promoter_transcript_id	Transcript_strand	CGI_Type	CGI_name (CpG:cpgNum:gcNum)	CGI_info (length;perCpg;perGc;obsExp)	Region	Gene
chr12-53931048	0.31	0.53	0.22	hyper	10	17	chr12	53931048	+	.	.	.	CGI_Shelf	CpG:41:278	420;19.5;66.2;0.9	intergenic	LOC107984525(dist=31981),HOXC13-AS(dist=4280)
chr12-53931051	0.46	0.71	0.24	hyper	10	17	chr12	53931051	+	.	.	.	CGI_Shelf	CpG:41:278	420;19.5;66.2;0.9	intergenic	LOC107984525(dist=31984),HOXC13-AS(dist=4277)
chr12-53931111	0.00	0.31	0.31	hyper	7	13	chr12	53931111	+	.	.	.	CGI_Shelf	CpG:41:278	420;19.5;66.2;0.9	intergenic	LOC107984525(dist=32044),HOXC13-AS(dist=4217)
chr12-53931140	0.50	0.79	0.29	hyper	6	14	chr12	53931140	-	.	.	.	CGI_Shelf	CpG:41:278	420;19.5;66.2;0.9	intergenic	LOC107984525(dist=32073),HOXC13-AS(dist=4188)
chr12-53935298	0.75	1.00	0.25	hyper	3	11	chr12	53935298	+	.	.	.	CGI_Shore	CpG:22:157	270;16.3;58.1;0.97	downstream	HOXC13-AS
chr12-53935516	0.40	0.64	0.24	hyper	12	14	chr12	53935516	-	.	.	.	CGI_Shore	CpG:22:157	270;16.3;58.1;0.97	ncRNA_exonic	HOXC13-AS
chr12-53935638	0.80	1.00	0.20	hyper	4	11	chr12	53935638	-	.	.	.	CGI	CpG:22:157	270;16.3;58.1;0.97	ncRNA_exonic	HOXC13-AS
chr12-53935732	0.67	1.00	0.33	hyper	7	14	chr12	53935732	-	.	.	.	CGI	CpG:22:157	270;16.3;58.1;0.97	ncRNA_exonic	HOXC13-AS
chr12-53935822	0.50	0.80	0.30	hyper	6	10	chr12	53935822	-	.	.	.	CGI	CpG:22:157	270;16.3;58.1;0.97	ncRNA_exonic	HOXC13-AS
chr12-53935837	0.63	0.90	0.28	hyper	6	10	chr12	53935837	-	.	.	.	CGI	CpG:22:157	270;16.3;58.1;0.97	ncRNA_exonic	HOXC13-AS
chr12-53937657	0.55	0.90	0.35	hyper	9	10	chr12	53937657	-	HOXC13	NM_017410	-	CGI_Shore	CpG:22:157	270;16.3;58.1;0.97	ncRNA_intronic	HOXC13-AS
chr12-53940553	0.60	0.92	0.32	hyper	4	12	chr12	53940553	+	HOXC13-AS	NR_047507	-	CGI_Shore	CpG:89:610	852;20.9;71.6;0.83	intronic	HOXC13
chr12-53943407	0.21	0.64	0.42	hyper	11	11	chr12	53943407	+	.	.	.	CGI_Shore	CpG:33:236	407;16.2;58;0.97	intronic	HOXC13
chr12-53944671	0.80	1.00	0.20	hyper	8	13	chr12	53944671	+	.	.	.	CGI_Shore	CpG:33:236	407;16.2;58;0.97	intronic	HOXC13
chr12-53944803	0.13	0.36	0.24	hyper	6	11	chr12	53944803	+	.	.	.	CGI_Shore	CpG:33:236	407;16.2;58;0.97	intronic	HOXC13
chr12-53951381	0.33	0.73	0.39	hyper	2	11	chr12	53951381	-	.	.	.	CGI_Shore	CpG:22:153	226;19.5;67.7;0.89	intergenic	HOXC13(dist=4837),LOC105369775(dist=2004)
chr12-53951386	0.33	0.91	0.58	hyper	2	11	chr12	53951386	-	.	.	.	CGI_Shore	CpG:22:153	226;19.5;67.7;0.89	intergenic	HOXC13(dist=4842),LOC105369775(dist=1999)
chr12-53952729	0.38	0.70	0.33	hyper	6	10	chr12	53952729	+	.	.	.	CGI_Shelf	CpG:22:153	226;19.5;67.7;0.89	downstream	LOC105369775
chr12-53958777	0.25	0.73	0.48	hyper	3	15	chr12	53958777	+	.	.	.	CGI_Shelf	CpG:80:454	683;23.4;66.5;1.06	UTR3	HOXC12
chr12-53958865	0.50	0.78	0.28	hyper	16	9	chr12	53958865	-	.	.	.	CGI_Shelf	CpG:80:454	683;23.4;66.5;1.06	UTR3	HOXC12
chr12-53958880	0.45	0.67	0.22	hyper	16	9	chr12	53958880	-	.	.	.	CGI_Shelf	CpG:80:454	683;23.4;66.5;1.06	UTR3	HOXC12
chr12-53960390	0.75	1.00	0.25	hyper	6	14	chr12	53960390	+	.	.	.	CGI_Shore	CpG:94:660	962;19.5;68.6;0.83	intergenic	HOXC12(dist=14341),HOTAIR(dist=1918)
chr12-53963731	0.20	0.60	0.40	hyper	4	10	chr12	53963731	-	.	.	.	CGI_Shelf	CpG:94:660	962;19.5;68.6;0.83	ncRNA_exonic	HOTAIR
chr12-53966478	0.57	1.00	0.43	hyper	11	13	chr12	53966478	+	.	.	.	CGI_Shore	CpG:18:147	248;14.5;59.3;0.83	ncRNA_intronic	HOTAIR
chr12-53967290	0.50	0.91	0.41	hyper	6	11	chr12	53967290	+	.	.	.	CGI_Shore	CpG:18:147	248;14.5;59.3;0.83	ncRNA_exonic	HOTAIR
chr12-53967637	0.60	0.86	0.26	hyper	8	14	chr12	53967637	+	.	.	.	CGI_Shore	CpG:18:147	248;14.5;59.3;0.83	ncRNA_intronic	HOTAIR
chr12-53968622	0.62	1.00	0.38	hyper	10	4	chr12	53968622	-	.	.	.	CGI_Shelf	CpG:18:147	248;14.5;59.3;0.83	ncRNA_exonic	HOTAIR
chr12-53981174	0.73	1.00	0.27	hyper	9	12	chr12	53981174	-	.	.	.	CGI_Shelf	CpG:112:905	1406;15.9;64.4;0.77	intergenic	HOXC11(dist=3531),HOXC-AS3(dist=2777)
chr12-53981316	0.38	0.75	0.37	hyper	10	8	chr12	53981316	-	.	.	.	CGI_Shelf	CpG:112:905	1406;15.9;64.4;0.77	intergenic	HOXC11(dist=3673),HOXC-AS3(dist=2635)
chr12-53982462	0.77	1.00	0.23	hyper	17	9	chr12	53982462	-	.	.	.	CGI_Shelf	CpG:112:905	1406;15.9;64.4;0.77	intergenic	HOXC11(dist=4819),HOXC-AS3(dist=1489)
chr12-53983049	0.64	0.86	0.21	hyper	11	7	chr12	53983049	+	.	.	.	CGI_Shore	CpG:112:905	1406;15.9;64.4;0.77	downstream	HOXC-AS3
chr12-53983558	0.75	1.00	0.25	hyper	3	11	chr12	53983558	-	HOXC10	NM_017409	+	CGI_Shore	CpG:112:905	1406;15.9;64.4;0.77	downstream	HOXC-AS3
chr12-53986563	0.75	1.00	0.25	hyper	6	12	chr12	53986563	-	HOXC-AS3	NR_047506	-	CGI_Shore	CpG:112:905	1406;15.9;64.4;0.77	intronic	HOXC10
chr12-53986940	0.69	1.00	0.31	hyper	10	4	chr12	53986940	+	HOXC-AS3	NR_047506	-	CGI_Shore	CpG:112:905	1406;15.9;64.4;0.77	intronic	HOXC10
chr12-53987289	0.75	1.00	0.25	hyper	3	12	chr12	53987289	+	HOXC-AS3	NR_047506	-	CGI_Shore	CpG:112:905	1406;15.9;64.4;0.77	intronic	HOXC10
chr12-53987858	0.50	0.80	0.30	hyper	5	10	chr12	53987858	-	.	.	.	CGI_Shore	CpG:112:905	1406;15.9;64.4;0.77	intronic	HOXC10
chr12-53991101	0.00	0.45	0.45	hyper	4	11	chr12	53991101	+	MIR196A2	NR_029617;ma-MIR196A2;ma-MIR196A2-2	+	CGI_Shelf	CpG:52:407	587;17.7;69.3;0.77	upstream;downstream	MIR196A2;HOXC10
chr12-53994303	0.33	0.70	0.37	hyper	2	10	chr12	53994303	+	.	.	.	CGI	CpG:52:407	587;17.7;69.3;0.77	downstream	HOXC-AS2
chr12-53994439	0.75	1.00	0.25	hyper	6	11	chr12	53994439	+	.	.	.	CGI	CpG:52:407	587;17.7;69.3;0.77	downstream	HOXC-AS2
chr12-53994511	0.67	1.00	0.33	hyper	7	10	chr12	53994511	+	.	.	.	CGI	CpG:52:407	587;17.7;69.3;0.77	downstream	HOXC-AS2
chr12-53995057	0.50	0.90	0.40	hyper	6	10	chr12	53995057	+	.	.	.	CGI_Shore	CpG:52:407	587;17.7;69.3;0.77	downstream	HOXC-AS2
chr12-54001026	0.57	0.78	0.21	hyper	11	9	chr12	54001026	+	HOXC-AS1	NR_047504	-	CGI_Shore	CpG:118:800	1274;18.5;62.8;0.94	intronic	HOXC9
chr12-54001902	0.71	1.00	0.29	hyper	11	4	chr12	54001902	+	HOXC-AS1	NR_047504	-	CGI_Shore	CpG:118:800	1274;18.5;62.8;0.94	intronic	HOXC9
chr12-54006335	0.00	0.25	0.25	hyper	2	16	chr12	54006335	+	.	.	.	CGI_Shore	CpG:26:160	242;21.5;66.1;1.02	intronic	LOC107984512
chr12-54006341	0.00	0.38	0.38	hyper	2	16	chr12	54006341	+	.	.	.	CGI_Shore	CpG:26:160	242;21.5;66.1;1.02	intronic	LOC107984512
chr12-54006507	0.40	0.63	0.23	hyper	12	16	chr12	54006507	+	.	.	.	CGI_Shore	CpG:26:160	242;21.5;66.1;1.02	exonic	LOC107984512
chr12-54006644	0.00	0.28	0.28	hyper	15	18	chr12	54006644	+	.	.	.	CGI_Shore	CpG:26:160	242;21.5;66.1;1.02	exonic	LOC107984512
chr12-54011092	0.77	1.00	0.23	hyper	17	13	chr12	54011092	+	.	.	.	CGI_Shore	CpG:49:351	665;14.7;52.8;1.06	exonic	HOXC8
chr12-54011710	0.56	0.80	0.24	hyper	14	10	chr12	54011710	+	.	.	.	CGI_Shelf	CpG:49:351	665;14.7;52.8;1.06	UTR3	HOXC8
chr12-54011786	0.00	0.23	0.23	hyper	11	13	chr12	54011786	+	.	.	.	CGI_Shelf	CpG:49:351	665;14.7;52.8;1.06	UTR3	HOXC8
chr12-54019950	0.67	0.92	0.25	hyper	7	12	chr12	54019950	-	.	.	.	CGI_Shore	CpG:30:230	356;16.9;64.6;0.81	intronic	HOXC4;HOXC6;HOXC5
chr12-54020489	0.77	1.00	0.23	hyper	10	7	chr12	54020489	+	.	.	.	CGI_Shore	CpG:30:230	356;16.9;64.6;0.81	intronic	HOXC4;HOXC6;HOXC5
chr12-54034640	0.75	1.00	0.25	hyper	3	10	chr12	54034649	-	.	.	.	CGI_Shelf	CpG:48:378	563;17.1;67.1;0.76	ncRNA_exonic	HOXC5
chr12-54037491	0.35	0.60	0.25	hyper	13	10	chr12	54037491	+	.	.	.	CGI_Shelf	CpG:126:1031	1684;15;61.2;0.8	intronic	HOXC4
chr12-54037782	0.77	1.00	0.23	hyper	10	9	chr12	54037782	+	.	.	.	CGI_Shelf	CpG:126:1031	1684;15;61.2;0.8	intronic	HOXC4
chr12-54038500	0.75	1.00	0.25	hyper	3	11	chr12	54038500	+	.	.	.	CGI_Shelf	CpG:126:1031	1684;15;61.2;0.8	intronic	HOXC4
chr12-54040606	0.77	1.00	0.23	hyper	10	8	chr12	54040606	-	.	.	.	.	.	.	intronic	HOXC4
chr12-54041186	0.60	0.83	0.23	hyper	8	12	chr12	54041186	+	.	.	.	.	.	.	intronic	HOXC4
chr12-54045234	0.33	0.54	0.21	hyper	2	13	chr12	54045234	+	.	.	.	CGI_Shore	CpG:79:581	901;17.5;64.5;0.85	intronic	HOXC4
chr12-54046226	0.63	0.90	0.28	hyper	6	10	chr12	54046226	-	.	.	.	CGI_Shore	CpG:79:581	901;17.5;64.5;0.85	intronic	HOXC4
chr12-54048077	0.25	0.91	0.66	hyper	3	11	chr12	54048077	+	.	.	.	CGI_Shore	CpG:79:581	901;17.5;64.5;0.85	intronic	HOXC4
chr12-54049175	0.60	1.00	0.40	hyper	4	11	chr12	54049175	-	.	.	.	CGI_Shore	CpG:79:581	901;17.5;64.5;0.85	intronic	HOXC4
chr12-54050817	0.24	0.56	0.33	hyper	13	16	chr12	54050817	+	.	.	.	CGI_Shelf	CpG:79:581	901;17.5;64.5;0.85	intronic	HOXC4

Supplementary Table S7. Eighty-one genes exhibiting the reduction of responsiveness to DHT in LNCaP-C9 cells.

ProbeID	GeneSymbol	LNCaP-V-signal	LNCaP-DHT-signal	LNCaP-C9-V-signal	LNCaP-C9-DHT-signal	LNCaP-V-flag	LNCaP-DHT-flag	LNCaP-C9-V-flag	LNCaP-C9-DHT-flag	LNCaP-DHT/V-Zscore	LNCaP-DHT/V-ratio	LNCaP-C9-DHT/V-Zscore	LNCaP-C9-DHT/V-ratio	ratio LNCaP/LNCaP-C9	GenbankAccession
A_21_P0012331	PSLNR	1309	31455	2442	25894	P	P	P	P	12.80	24.03	11.45	10.60	2.3	NR_132385
A_23_P29067	TMPRSS2	456	9140	263	2227	P	P	P	P	11.26	20.02	7.99	8.46	2.4	NM_005656
A_21_P0011196		128	2828	263	2437	P	P	P	P	10.48	22.16	8.34	9.27	2.4	
A_33_P3378659	TARP	109	1655	120	691	P	P	P	P	9.22	15.24	5.71	5.76	2.6	NM_001003799
A_24_P5750	KLK2	1045	10030	2478	9643	P	P	P	P	8.49	9.60	6.59	3.89	2.5	NM_005551
A_22_P0001744	CENPN	538	4509	595	1628	P	P	P	P	7.99	8.38	3.76	2.74	3.1	NM_001100624
A_23_P359277	ELOVL7	186	1826	183	889	P	P	P	P	7.73	9.84	5.91	4.85	2.0	NM_024930
A_33_P3223501	PHGR1	184	1046	40	103	P	P	P	P	5.88	5.69	2.21	2.59	2.2	NM_001145643
A_23_P252201	EAF2	150	686	175	406	P	P	P	P	5.15	4.58	2.77	2.33	2.0	NM_018456
A_23_P68740	CENPN	2337	8187	3410	5767	P	P	P	P	5.04	3.50	2.54	1.69	2.1	NM_018455
A_21_P0014553	DUXAP9	407	1719	578	1339	P	P	P	P	4.87	4.22	3.14	2.32	1.8	BC013393
A_24_P189533	ENDOD1	1940	6794	1816	3349	P	P	P	P	4.71	3.50	2.63	1.84	1.9	NM_015236
A_23_P134935	DUSP4	637	2156	543	813	P	P	P	P	4.58	3.38	1.51	1.50	2.3	NM_001394
A_33_P3276703	VGF	352	1202	939	1913	P	P	P	P	4.15	3.41	3.05	2.04	1.7	NM_003378
A_23_P160460	UAP1	1840	5354	2918	5104	P	P	P	P	4.01	2.91	2.40	1.75	1.7	NM_003115
A_23_P52939	SLC43A1	656	1790	1162	1678	P	P	P	P	3.77	2.73	1.58	1.44	1.9	NM_003627
A_23_P133438	OTULINL	104	392	156	267	P	P	P	P	3.72	3.79	1.74	1.71	2.2	NM_019018
A_33_P3273719	ELOVL5	135	460	123	249	P	P	P	P	3.42	3.41	2.31	2.03	1.7	NM_001242831
A_33_P3254335	BEND4	249	682	244	413	P	P	P	P	3.41	2.74	1.96	1.69	1.6	NM_001159521
A_23_P204847	LCP1	686	1687	622	884	P	P	P	P	3.38	2.46	1.31	1.42	1.7	NM_002298
A_33_P3254634	PDIA5	166	450	227	407	P	P	P	P	3.38	2.71	2.17	1.79	1.5	NM_006810
A_33_P3387601	KLKP1	123	398	125	261	P	P	P	P	3.28	3.24	2.41	2.09	1.5	NR_002768
A_24_P166613	EPDR1	228	584	279	441	P	P	P	P	3.18	2.56	1.71	1.58	1.6	NM_017549
A_33_P3282614	STPG3	232	586	258	349	P	P	P	P	3.14	2.53	1.11	1.35	1.9	NM_001164489
A_32_P71447	NCAPD3	869	1968	1113	1443	P	P	P	P	3.07	2.27	1.12	1.30	1.7	NM_015261
A_23_P148297	SH3BGRL	874	1898	1612	2111	P	P	P	P	2.92	2.17	1.17	1.31	1.7	NM_003022
A_23_P119778	SLC39A10	623	1443	872	1288	P	P	P	P	2.89	2.35	1.45	1.48	1.6	NM_020342
A_19_P0320729	COYL2	855	1835	871	1158	P	P	P	P	2.87	2.15	1.06	1.33	1.6	NM_152342
A_23_P46110	TSC2	850	1803	1044	1329	P	P	P	P	2.83	2.12	1.05	1.27	1.7	NM_000548
A_32_P517749	RPS6KA3	574	1180	849	1113	P	P	P	P	2.44	2.06	1.00	1.31	1.6	XM_017029716
A_24_P404245	PCYT2	284	583	329	445	P	P	P	P	2.43	2.05	1.12	1.35	1.5	NM_002861
A_23_P13907	IGF1	102	216	169	220	P	P	P	P	2.11	2.13	0.87	1.30	1.6	NM_000618
A_33_P3332126	SCLY	106	224	234	279	P	P	P	P	2.10	2.12	0.58	1.19	1.8	AY127329
A_33_P3227904	SLC25A34	181	87	32	23	P	P	P	P	-2.05	0.48	-0.71	0.74	0.6	NM_207348
A_23_P390148	RALGPS1	213	100	160	123	P	P	P	P	-2.11	0.47	-0.86	0.77	0.6	NM_014636
A_23_P350187	TET2	169	79	86	62	P	P	P	P	-2.12	0.47	-0.77	0.72	0.7	NM_001127208
A_24_P391568	ARNT	167	78	126	104	P	P	P	P	-2.12	0.47	-0.62	0.83	0.6	NM_001668
A_33_P3230244	CSMD1	217	100	105	73	P	P	P	P	-2.15	0.46	-1.17	0.70	0.7	NM_033225
A_33_P3338121	LAMB3	111	51	28	25	P	P	P	P	-2.17	0.46	-0.23	0.91	0.5	NM_000228
A_33_P3303104	MYNN	244	112	119	121	P	P	P	P	-2.17	0.46	0.07	1.02	0.4	NM_001195119
A_21_P014244	ENPP5	370	166	163	85	P	P	P	P	-2.22	0.45	-0.62	0.83	0.5	NM_021572
A_33_P3213772	SRGAP2	186	79	109	89	P	P	P	P	-2.38	0.43	-0.45	0.82	0.5	NM_001300952
A_23_P93141	GSTA5	490	241	249	207	P	P	P	P	-2.40	0.49	-0.60	0.83	0.6	NM_153699
A_23_P376188	BEND7	167	70	248	172	P	P	P	P	-2.41	0.42	-1.18	0.69	0.6	NM_001169863
A_33_P3290562	GLI3	255	107	123	111	P	P	P	P	-2.42	0.42	-0.32	0.91	0.5	NM_000168
A_23_P109819	EPHA3	290	119	417	280	P	P	P	P	-2.47	0.41	-1.50	0.67	0.6	NM_005233
A_33_P3381378	PAX1	221	91	106	68	P	P	P	P	-2.48	0.41	-1.43	0.64	0.6	NM_001257096
A_32_P109604	ANKRD20A12P	184	74	102	96	P	P	P	P	-2.53	0.40	-0.20	0.94	0.4	NR_046228
A_23_P211212	COL18A1	441	208	1046	749	P	P	P	P	-2.53	0.47	-1.26	0.72	0.7	NM_030582
A_23_P105862	FRY	507	237	790	622	P	P	P	P	-2.57	0.47	-0.91	0.79	0.6	XM_017020306
A_21_P0010650	LOC102723382	278	104	149	116	P	P	P	P	-2.75	0.37	-0.81	0.78	0.5	XR_002958891
A_24_P203964	GUSBP14	1204	534	912	623	P	P	P	P	-2.75	0.44	-1.44	0.68	0.6	NR_024426
A_33_P3593774	PIK3R3	297	109	152	88	P	P	P	P	-2.79	0.37	-1.75	0.58	0.6	NM_003629
A_24_P411899	RNF19A	232	84	204	133	P	P	P	P	-2.82	0.36	-1.38	0.65	0.6	NM_183415
A_32_P140706	PMS2	655	282	405	314	P	P	P	P	-2.85	0.43	-0.97	0.77	0.6	NM_000535
A_24_P393958	DNAJB4	130	45	105	55	P	P	P	P	-2.93	0.35	-1.50	0.52	0.7	NM_007034
A_33_P3256113	GUSBP1	225	76	177	93	P	P	P	P	-3.02	0.34	-2.10	0.52	0.6	NR_027026
A_23_P134755	TRPS1	338	113	336	189	P	P	P	P	-3.05	0.33	-1.86	0.56	0.6	NM_014112
A_21_P0007223	LINC02614	201	64	147	74	P	P	P	P	-3.16	0.32	-2.21	0.51	0.6	NR_125395
A_24_P411749	ADGRG6	2988	1261	7058	5544	P	P	P	P	-3.24	0.42	-1.18	0.79	0.5	NM_020455
A_22_P00011829	SCAT8	154	44	41	29	P	P	P	P	-3.46	0.29	-0.85	0.69	0.4	NR_157886
A_32_P208120	CAMKID	182	51	188	91	P	P	P	P	-3.53	0.28	-2.37	0.48	0.6	NM_153498
A_23_P108444	MT2A	10413	4312	5845	3878	P	P	P	P	-3.55	0.41	-2.00	0.66	0.6	NM_005953
A_32_P95462	STXBP5L	293	81	220	139	P	P	P	P	-3.57	0.28	-1.50	0.63	0.4	NM_001348343
A_24_P268786	MYNN	1088	348	453	349	P	P	P	P	-3.86	0.32	-1.00	0.77	0.4	NM_018557
A_23_P418785	STXBP5L	1602	305	751	444	P	P	P	P	-4.02	0.30	-1.98	0.59	0.5	NM_001348343
A_24_P319923	MYLK	154	26	68	45	P	P	P	P	-4.04	0.17	-0.99	0.65	0.3	NM_053025
A_32_P25437	SLC13A2	1418	429	718	605	P	P	P	P	-4.05	0.30	-2.16	0.56	0.5	NM_001040
A_23_P380181	LMO4	3405	1143	1355	709	P	P	P	P	-4.10	0.34	-2.44	0.52	0.6	NM_006769
A_24_P211565	C1QTNF6	164	37	113	56	P	P	P	P	-4.18	0.22	-1.62	0.50	0.4	NM_031910
A_33_P3298425	LMO4	2322	743	894	469	P	P	P	P	-4.27	0.32	-2.43	0.52	0.6	NM_006769
A_23_P1668	MYLK	326	68	187	104	P	P	P	P	-4.37	0.21	-1.91	0.56	0.4	NM_053026
A_24_P49260	SPTLC3	379	79	657	221	P	P	P	P	-4.38	0.21	-4.10	0.34	0.6	NM_018327
A_23_P58407	UGT2B15	3451	965	3623	1578	P	P	P	P	-4.78	0.28	-3.53	0.44	0.6	NM_001076
A_23_P131676	ACKR3	17385	5263	20502	11406	P	P	P	P	-4.81	0.30	-3.84	0.56	0.5	NM_020311
A_23_P140831	AMIGO2	192	22	222	44	P	P	P	P	-4.83	0.12	-5.24	0.20	0.6	NM_181847
A_23_P62932	ATP1B1	10613	3170	8822	4029	P	P	P	P	-4.87	0.30	-3.81	0.46	0.7	J03779
A_33_P3398864	ZNF792	136	15	27	27	P	A	P	P	-4.89	0.11	-0.06	0.98	0.1	NM_175872
A_23_P160318	COL16A1	554	67	204	42	P	P	P	P	-5.90	0.12	-5.13	0.21	0.6	NM_001856
A_33_P3303414	MAN1A1	132	9	90	11	P	A	P	A	-6.14	0.07	-4.81	0.13	0.5	NM_005907
A_33_P3356935	COLCA1	3657	653	2902	813	P	P	P	P	-6.47	0.18	-5.40	0.28	0.6	NM_207326

Supplementary Table S8. gRNA sequences.

gRNA	Sequence
gRNA-1	agcatgaaaaataaatgcaa
gRNA-2	agcgcgtaattaacacaaaa
gRNA-3	cccctgcttcccagtcagcg
gRNA-4	caaattcccaaccgtttcat

Supplementary Table S9. Primer sets used for the GeneArt Genomic Cleavage Detection (GCD) experiment, PCR product size, and digested DNA fragments by GCD detection enzyme.

GCD Primer	Forward	Reverse	PCR Product (bp)	Digested by GCD enzyme (bp)
gRNA-1-GCD	gcaaccgcatgttgagtcta	tctgtccctctggtttggtc	533	219+314
gRNA-2-GCD	gcgctgttgctcaatgttag	gggctttgtgtcttggaatg	600	295+305
gRNA-3-GCD	gaattacagccctcccgaac	ccccacttttatccccactt	527	149+378
gRNA-4-GCD	agacttttcccgtctcagca	cagcccaggacttctgctac	520	248+272